Desalination and Water Treatment 324 (2025) 101576

Contents lists available at ScienceDirect

Desalination and Water Treatment

journal homepage: www.sciencedirect.com/journal/desalination-and-water-treatment/

Dewatered sewage sludge textural and viscoelastic changes during its drying: Focus on the sticky phase

Sergio Luis Parra-Angarita [a,*], Mohamed Essanoussi [b], Hajer Ben Hamed [a], Azeddine Fantasse [a], Angélique Léonard [a,*]

[a] Chemical Engineering Research Unit, PEPs, University of Liège, Liège 4000, Belgium
[b] Sciences et Techniques, Haute École de la province Liège, Liège 4000, Belgium

ARTICLE INFO

Keywords:
Sewage Sludge
Sticky Phase
Drying Behaviour
Texture
Viscoelasticity

ABSTRACT

This study characterizes viscoelastic and textural evolution of dewatered sewage sludge (DSS) during thermal drying, with a particular focus on identifying the moisture ranges associated with its sticky-phase (S-P). DSS samples were collected from three wastewater treatment plants and analysed for total solids (TSC) and volatile solids (VS). Samples were dried in 100 g batches at 105 °C and tested at discrete moisture levels. Samples were homogenized and extruded into cylinders measuring 3 cm in height and 1.5 cm in diameter. The samples were analysed using texture profile analysis, rheology, penetrometry, and X-ray microtomography; tests were done by triplicate to ensure reproducibility. For all samples, the sticky phase was identified between 20 $\%_{DS}$ and 35 $\%_{DS}$, a range consistently confirmed across methods, by a peak in the adhesiveness-to-cohesiveness (A/C) ratio in TPA and penetrometry, a stabilization of the storage modulus (G′) in rheology, and a drop in porosity by micro-tomography This convergence indicates that the sticky phase represents a critical transition between viscoelastic-pasty and viscoelastic-solid states, associated with internal structural rearrangement and moisture redistribution The proposed multi-technique methodology can be adapted to other sludge types to map their sticky phase and to support the design and optimization of drying operations.

1. Introduction

According to the European Statistical Office (Eurostat), over 80 % of the European population is connected to wastewater treatment plants (WWTPs). WWTPs consist of a series of well-defined stages involving physical, chemical, and microbiological processes to remove contaminants as shown in Fig. 1. These processes produce sewage sludge, a complex mixture comprising microorganisms, traces of inorganic matter, and occasional pollutants derived from human waste. In the last decade, in Europe sludge production has reached a stable plateau value production of 10 million tons per year, measured as total solid content, which poses significant environmental and operational challenges for ensuring proper sludge management and final disposal [1,2].

Sewage sludge requires specific treatment steps within WWTPs, including thickening, dewatering, stabilization (e.g., anaerobic digestion or liming), and drying, each aiming to reduce volume, stabilize organic matter, and prepare sludge for final disposal or valorisation. These operations are shown in yellow, orange, and grey in Fig. 1. In fact, sludge management can account for 20–65 % of the total operating costs of WWTPs [3], while thermal drying alone can represent 50–70 % of the total energy consumption of the sludge line [4]. These figures underscore the importance of optimizing sludge drying processes, which depend heavily on understanding the material's changing physical behaviour during drying

Throughout treatment line, sludge undergoes a transition from a Newtonian liquid to a pasty soft solid and to a dry Solid and finally to a dry solid when thermal drying is applied. sludge obtained from primary to tertiary treatment behaves as Newtonian liquid (total solid content or TSC from 0.2 % to 1 % of dry solids or $\%_{DS}$), then the after its thickening it becomes a highly viscous non-Newtonian liquid, saturated of dissolved and suspended solids (TSC from 1 % to 10 $\%_{DS}$) [5,6]. After mechanical dewatering, the sludge is transformed into a mud-like substance also known as dehydrated sewage sludge (DSS) (TSC from 10 % to 45 $\%_{DS}$), which behaves as a gel or a soft solid [7–11]. Finally, in the case of a drying treatment, DSS gets a granular, solid phase [12–14] (TSC $>$ 90 $\%_{DS}$). Fig. 1 also shows the process diagram of a general

* Corresponding authors.
E-mail addresses: slparra@uliege.be (S.L. Parra-Angarita), a.leonard@uliege.be (A. Léonard).

https://doi.org/10.1016/j.dwt.2025.101576
Received 27 August 2025; Received in revised form 14 November 2025; Accepted 20 November 2025
Available online 21 November 2025

WWTP and the corresponding sludge phase at each step.

Drying is a critical step in sludge treatment, reducing volume, increasing stability, and preparing the sludge for further use [16]. It is energy-intensive, and its performance is strongly influenced by the textural and viscoelastic properties of DSS, which depend on its origin, treatment conditions, and other variables [17]. During the thermal drying of DSS, a challenging phase commonly referred to as the sticky phase (S-P) emerges at intermediate moisture contents. In this stage, sludge exhibits a highly cohesive, plastic-rubbery behaviour that significantly complicates drying operations due to strong adhesion to dryer surfaces and altered flow dynamics. This phenomenon reduces dryer efficiency and increases operational instability. Stickiness is primarily attributed to the interaction between organic matter (such as proteins and polysaccharides) and moisture, which governs the rheological properties of DSS [18,19]. The S-P typically occurs within a moisture content range of 30–65 %DS, as shown in Table 1.

Characterization of S-P is complex due to the lack of standardized methods, though analogies with soil mechanics have been proposed to identify critical transitions from liquid to plastic and plastic to solid states. Table 1 presents a summary of key studies that have investigated the sticky phase of sewage and faecal sludge during drying. Each entry includes the reported interval for the sticky phase, a brief description of the sludge origin, and the measurement method used. This overview highlights the diversity of experimental approaches and sludge types analysed in the literature, offering valuable context for comparing results across different conditions and research objectives.

As shown in Table 1, a clear and standardized approach for identifying the sticky phase (S-P) is still lacking. Reported intervals vary widely across studies, often due to differences in sludge origin, pretreatment, and measurement technique. Moreover, many studies rely on a single analytical method, which may overlook the complex, multiparameter nature of stickiness. There is therefore a strong need for integrative studies using multiple methods to provide converging evidence and a more robust characterization of the S-P in real DSS samples.

This study aims to advance current understanding of the S-P during sludge drying by exploring the viscoelastic and textural transitions of real DSS samples across a wide range of moisture contents. Beyond identifying the moisture range where the S-P occurs, this work complements existing knowledge by introducing and validating alternative methods for characterizing this complex behaviour. By combining established and novel measurement techniques, this work provides new insights and practical approaches for optimizing DSS drying processes under different treatment conditions.

2. Materials and methods

2.1. Dehydrated sewage sludge samples

DSS samples were collected from three WWTPs in the Liège region (Belgium): Embourg (Em), Grosses-Battes (Gb), and Oupeye (Ou). Each sample was stored at 4 °C for a maximum of five days throughout the experimental period to prevent biochemical activity and loss of integrity y [28].

2.2. Total solid content and volatile solids content

The total solid content (TSC) and volatile solids content (VS) were measured according to standard methods [29]. For TSC determination, samples were dried at 105 °C until a stable weight was reached. To assess VS, the dried samples were then subjected to calcination at 550 °C for two hours, and the organic matter content was estimated based on the resulting mass loss. TSC is expressed in $\%_{DS}$ and VS as %TSC.

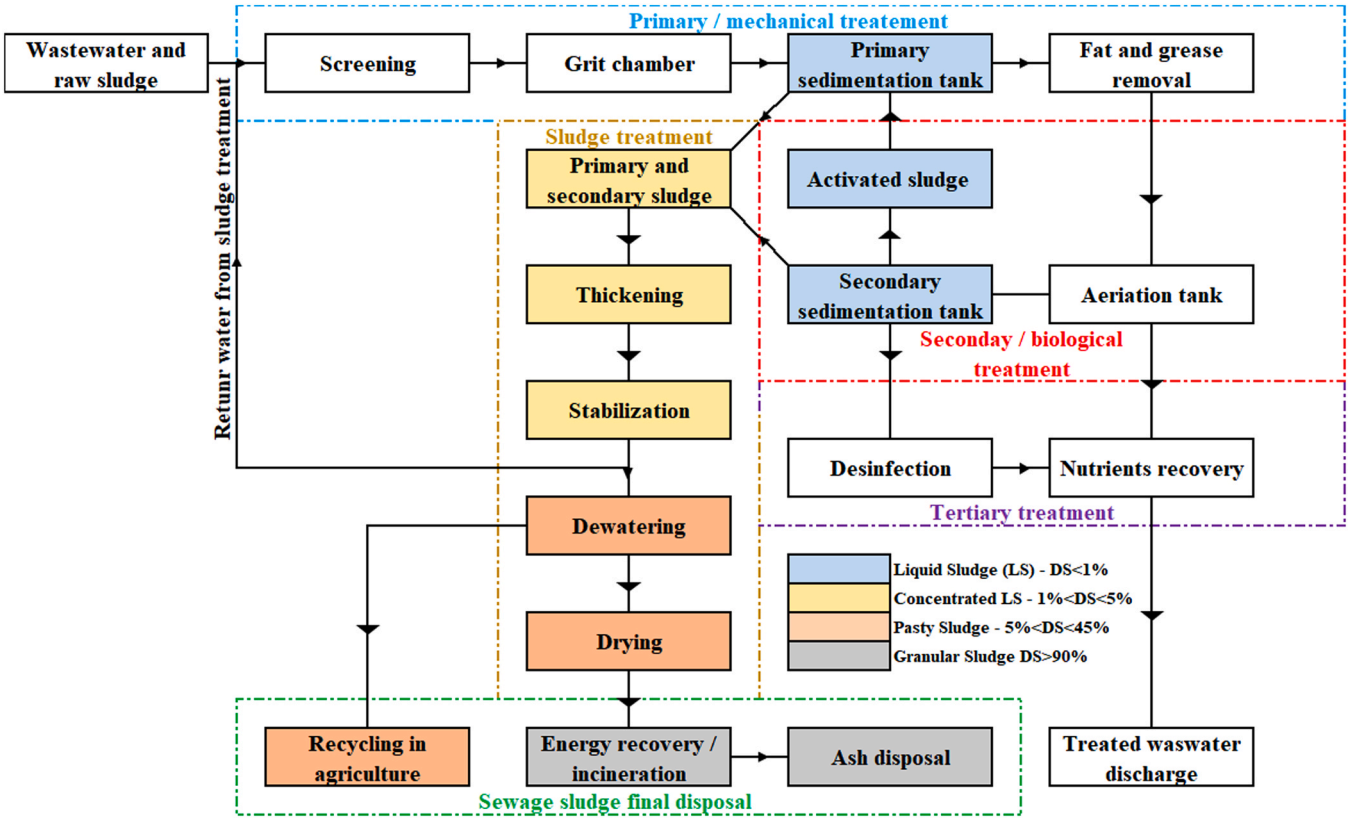

Fig. 1. Sewage sludge phases through a waste water treatment plant.
(adapted from [15]).

Table 1
Reported sticky phase intervals of sewage and faecal sludge in drying processes.

Reference	Sticky Phase Interval ($\%_{DS}$)	Sludge Origin Description	Measuring Method
[20]	30–65	Digested SS	Continuous torque measurement device on agitated activated sludge while being dried.
[21]	25–75	Municipal DSS	Measure of the mechanical torque necessary for stirring in a batch dryer
[22]	40–80	Municipal DSS	The consistency limits (liquidity and plasticity) were determined using standardised soil mechanics trials based on Atterberg's limits
[10]	35–60	Industrial DSS	Adapted soil shear test protocol
[23]	35–45	Industrial DSS	Scraping test simulating dryer operation
[12]	50–65	Municipal DSS	Modified Peeters Shear test protocol
[24]	45–55	Municipal DSS	Modified Peeters Shear test protocol and agitated drying with torque measurement
[25]	30–60	Municipal DSS with varying CaO additions	Custom device: tensile, shear and compression stress under varying temperature and
[26,27]	30–60	Faecal sludge from VIP and UDDT toilets (South Africa)	Compression test and Oscillatory Rheology
[19]	40–50	Municipal DSS with high sand content	Adhesion and cohesion tests under varying sand/temp conditions

2.3. Dehydrated sewage sludge drying

Samples were manually extruded through a circular die with 12 mm openings. A reference drying curve was established using three aluminium crucibles (75 mm diameter, 30 mm height), each containing approximately 100 g of DSS. The crucibles were placed in a laboratory oven set at a constant temperature of 105 °C. Over a 24-hour period, samples were weighed each 30 min. At each interval, the mass of each crucible was recorded individually, and the values were averaged to minimize the influence of initial mass differences. These averages were used to construct the drying curve over time.

2.4. Tracking of the evolution of textural and viscoelastic properties during drying

To follow the evolution of textural and viscoelastic properties during drying, DSS samples were dried under the conditions described in Section 2.3. Each sample was removed at every increment of 5 % in TSC from the dryer, which was estimated using the reference drying curve obtained from a blank test.

After reaching the target TSC, each aluminium container was individually processed. To ensure sample consistency and remove the dry crust formed on the outer surface during drying, the sludge was homogenized using a mortar and pestle before testing. Although this mechanical homogenization may slightly modify the natural texture of DSS, the procedure was applied consistently to all samples using the same operator, duration, and tools to ensure comparability. This methodological step was adapted from the word of Peeters et al. [10] which is commonly used in similar studies involving rheological and textural characterization of complex sludge-like materials [19,27].

- Penetration test

Penetrometry and Texture profile analysis (TPA) tests were conducted using a universal testing machine (LS1, AMETEK Lloyd Instruments, UK) equipped with 10 N or 100 N load cells, depending on sample firmness. A 30 mm spherical probe was used for penetration, and a 60 mm flat plate for TPA. A 60 g portion of DSS was placed into an aluminium container and subjected to a penetration test using a spherical probe. The probe was inserted vertically into the sample to a depth of 10 mm at a constant speed of 1 mm/s. After reaching the target depth, the probe remained in place for one minute before being withdrawn at the same constant speed, this methodology was adapted from the work done by Pambou Y. in his PhD theses [30]. Each measurement was performed in triplicate.

- Texture profile analysis test

  Samples were extruded into cylinders measuring 18 mm in diameter and 30 mm in height. The samples were subjected to a dual-round compression test using a flat circular head with a diameter of 60 mm. The compression was performed to achieve 30 % of the original sample height at a constant speed of 1 mm/s, these parameters were adopted following previous work on sludge texture behaviour [11,31]. This testing protocol is crucial for evaluating how the material behaves under pressure, providing valuable data on its hardness, cohesiveness, and adhesiveness. These properties are essential for understanding the structural integrity and processing suitability of DSS. Measurements were performed in triplicate.
- Oscillatory rheology test

  Oscillatory rheology measurements were carried out using an MCR302e rheometer (Anton Paar, Austria) with a 50 mm serrated parallel plate. All tests were conducted at 20 °C to prevent moisture loss, and data were acquired using RheoCompass v1.30® software. Tests were performed with logarithmic shear strain ramp from 0.01 % to 1000 % at a constant angular frequency of 1 Hz. To maintain consistency in sample conditions, a pre-shearing process was instituted for 1 min at a shear rate of 0.05 % and frequency of 1 Hz, followed by a 10-minute rest period before measurements [14]. Measurement was performed in triplicate.

  As expected, the sample structure was completely disrupted beyond 100 % strain. This wide amplitude range was intentionally used to capture the full viscoelastic response of the dehydrated sewage sludge (DSS) and to identify the limit of the LVER. Only values within the LVER were considered for further analysis. The determination of the LVER was performed using the *"Limit LVER"* macro available in the Anton Paar RheoCompass v1.30® software, which automatically calculates the linear viscoelastic domain using smoothed G' data as a function of shear strain (γ) with a 3 % tolerance band. The representative G' values reported in this study correspond to the mean values within the LVER range, typically between 0.1 % and 1 % strain depending on the TSC of the sample.
- Microtomography reconstruction

The X-ray tomography was performed by using a Skyscan-1074 X-ray system (Skyscan, Ghent, Belgium). The scans, with a pixel resolution of 41 μm, were reconstructed using Skyscan/NRecon V1.7.4.2; image analysis was then performed in Matlab 2020® to determine the average closed porosity (i.e., free volume) of the samples, expressed as a percentage. The cylindrical DSS sample (15 mm diameter × 30 mm height) obtained at each point of the tracking was monitored using X-ray microtomography. The sample was periodically removed from the dryer and scanned for approximately 3, capturing multiple cross-sectional images. Only one scan per %TSC was acquired per experimental run, due to the time required for acquisition and processing. However, an as mentioned IN Section 2.4, the full drying protocol, including tomography, was independently replicated for each of the three WWTPs studied, ensuring the reproducibility of observed trends.

As such, although no replicate scans were taken at each TSC point, the micro-CT results are considered qualitative yet complementary,

providing structural insight into the evolution of porosity during drying across real DSS samples.

3. Results

3.1. General differences between samples

The origin of the DSS plays a crucial role in its rheological and textural behaviour throughout drying [31]. Table 2 summarizes relevant characteristics of the WWTPs included in this study, such as capacity and commissioning year, type of treatment, which may influence DSS properties, even when treatment types appear similar. The ✔ and ✖ symbols reflect the presence or absence of specific treatments at each plant respectively.

TSC provides insight into initial moisture and the minimum mass achievable through conductive drying, as well as the efficiency of each plant's dewatering process. Among the samples, TSC ranged from 14.01 % to 20.86 $\%_{DS}$ (Before liming). VS, associated with the organic fraction of the DSS and its potential agricultural value, varied depending on liming. As expected, lime sample had lower VS (<60 %), while non-limed samples exceeded 60 %, classifying them as organic DSS. In total, four samples were analysed: three non-limed and one limed. Notably, the Gb sample was available in both its raw and limed forms, allowing for direct comparison.

3.2. DSS evolution of textural and viscoelastic properties during drying

The penetration test, the TPA test and the oscillatory rheology test are essential for assessing the mechanical behaviour of DSS samples [5, 32,33], The general obtained results and the standard graphical output from mentioned tests can be found in the literature [31].

- **Texture profile analysis test**

Table 2
Highlights of the WWTPs considered in the study and TSC and VS of DSS samples.

Feature	Embourg	Oupeye	Grosses - Battes	
Code	Em	Ou	Gb / Gb_L	
Capacity [PE]	24,300	402,000	53,100	
Commissioning	1996	2007	2002	
Water treatment		Activated sludge		
P/C/N removal	✔	✔	✔	
Sludge stabilization	Liming*	Anaerobic digestion	Liming	
Sludge thickening	✔	✖	✖	
Dewatering technology	Belt Filter	Centrifugation	Belt Filter	
Liming	✖	✖	✔ / ✖	
Carbon treatment	✔	✔	✔	
Nitrogen treatment	✔	✔	✔	
Bacteriological treatment	✖	✖	✖	
Final disposition	Incineration	Incineration	Agriculture / Incineration	
TSC and VS of DSS samples				
TSC [$\%_{DS}$]	18.87 ± 0.01	20.86 ± 0.03	14.01± 0.01	17.57 ± 0.07
VS [%TSC]	66.8 ± 0.3	66.8 ± 0.5	72.5 ± 0.1	56.9 ± 0.5

* Sludge is limed after being dehydrated in an external installation.

TPA parameters tracked during the drying of DSS included adhesiveness, cohesiveness. adhesiveness reflects the sample's tendency to stick to the probe, and cohesiveness corresponds to the sample's ability to deform and return to its original shape [34].

As drying progressed, DSS hardness increases with total solid content, requiring more force to compress. This increase impacts both cohesiveness and adhesiveness. While adhesiveness tends to rise slightly, the change is modest compared to the increase in cohesiveness. To assess the balance between these properties, the adhesiveness-to-cohesiveness ratio (A/C) was calculated.

Fig. 2 shows the obtained curves of A/C ratio across drying for samples Em, Ou and Gb revealed a distinct S-P occurring between 20 % and 30 $\%_{DS}$. In this range, each sample exhibited a sharp increase in the A/C ratio, followed by a peak and then a steep drop, eventually stabilizing at higher dryness levels. The variation in peak positions among samples suggests that the sticky behaviour is influenced by the DSS's initial composition. Unfortunately, the TPA test was not useful for TSC bigger than 45 %, giving the partially destruction of the samples structure.

Error bars in Fig. 2 represent the standard deviation from triplicate measurements at each moisture level. Across all DSS samples, standard deviations remained below 5 % for both adhesiveness and cohesiveness, highlighting the high reproducibility of the TPA measurements despite the complex and heterogeneous nature of the material [28].

Comparing samples Gb and Gb_L highlights the effect of liming on stickiness. The limed sample Gb_L showed a lower overall A/C ratio and a shift of the S-P peak toward lower dryness. This behaviour suggests that lime alters the DSS's microstructure and water distribution, reducing its adhesion to surfaces. The faster drop in the A/C ratio for Gb_L also indicates a less stable S-P. These findings align with drying tests, where liming promoted rigidity. Although this effect can be further optimized, lime addition appears to mitigate stickiness during DSS drying.

- Penetration test

Penetrometry parameters tracked during DSS drying included penetration work and withdrawal work. The penetration work, defined as the area under the force–displacement curve during the insertion of the probe, is associated with the sample's cohesiveness, reflecting the internal resistance to deformation and structural integrity. The withdrawal work, corresponding to the area under the curve as the probe is retracted, is linked to the sample's adhesiveness, representing its tendency to stick to surfaces [31]. These two parameters together allow for a mechanical characterization of the sludge's transition from soft, sticky

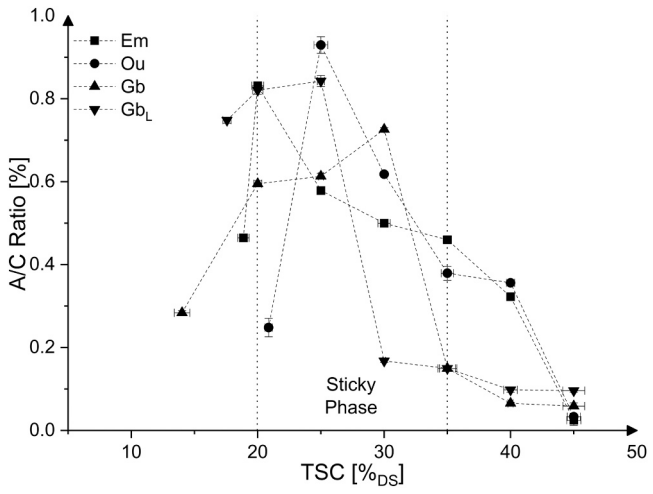

Fig. 2. Evolution of the adhesiveness-to-cohesiveness ratio from TPA during drying of DSS samples.

behaviour to a more rigid and dry state during the drying process.

The A/C ratio curves obtained from the penetrometry tests during drying are presented in Fig. 3. All four curves indicate the presence of a characteristic S-P also occurs between 20 % and 35 $\%_{DS}$. Within this range, each sample exhibits a distinct peak in the adhesiveness-to-cohesiveness ratio, with slight variations in peak position, suggesting that stickiness is influenced by the DSS's initial composition or origin. A consistent trend is observed across all samples: a rapid rise in the ratio, a pronounced peak, a sharp decline, and finally a plateau as drying progresses.

Overall, the limed sample (Gb_L) exhibited a lower A/C ratio across the entire dryness range, Aligning results with the literature. The sharper decline in this ratio suggests a less stable S-P. Liming appears to enhance DSS rigidity and promote free water release, as also confirmed by the drying tests. While the effect may be further optimized, lime addition shows promise in reducing adhesiveness during drying. In contrast to TPA, the penetration test proved suitable across the entire drying range for DSS

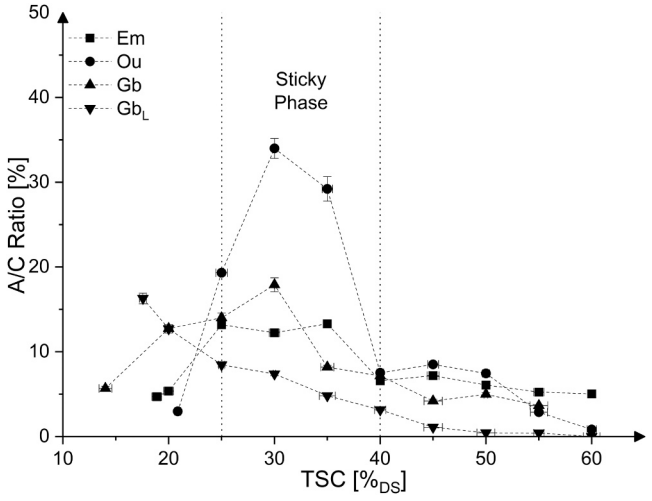

Fig. 3. Evolution of the adhesiveness-to-cohesiveness ratio from penetration tests during drying of DSS samples.

3.3. Oscillatory rheology test

Rheological parameters tracked during DSS drying included the storage modulus (G′) and the loss modulus (G″). G′ represents the elastic component of the material, indicating the ability of the sludge to store mechanical energy during deformation, while the G″ corresponds to the viscous component, describing the energy dissipated as internal friction [35]. As drying progresses, the increase of G′ over G″ marks the transition from a viscous, gel-like behaviour to a more elastic, solid-like structure.

As expected, and in agreement with the literature, G′ at the limit of the viscoelastic region increased progressively throughout the drying process of the DSS samples as show in Fig. 4 [36,37]. However, a notable stabilization of this parameter was observed between 25 % and 30 $\%_{DS}$ for all samples, except for Gb_L. Interestingly, this interval corresponds closely with the S-P ranges identified through penetrometry and TPA.

During the laboratory tests, it was observed that once the TSC reached around 40 %, the DSS samples began forming cylindrical shapes that rolled and stuck to themselves while detaching from the rheometer's measuring plate. This behaviour altered the measurement area and suggests that cohesive forces begin to dominate over adhesive ones at this moisture level, a phenomenon previously reported by various researchers.

Under the experimental conditions used in this study, oscillatory rheology is not recommended for samples with TSC greater than 50 $\%_{DS}$,

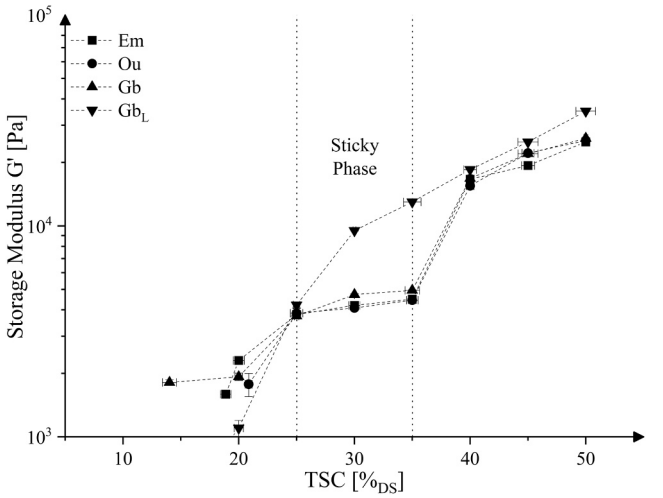

Fig. 4. Evolution of storage modulus from oscillatory rheology test during drying of DSS samples.

as the presence of solids may damage the measuring device and interfere with reliable data acquisition. For TSC values above this threshold, we recommend using a granular rheometer or dry-material rheology setup [13].

- Microtomography reconstruction

X-ray microtomography was used to monitor the internal structure and porosity evolution of DSS samples during drying. The analysis focused specifically on closed porosity, defined as the internal void fraction not connected to the exterior surface. Changes in closed porosity reflect structural rearrangements in the sludge matrix as moisture is removed. As drying progresses, pore shrinkage, collapse of floc structures, and densification occur, leading to a gradual reduction in the detected free volume [38].

The obtained cross sections obtained from the microtomography reconstruction allowed us to follow the enclosed porosity of the sludge samples during is drying, in Fig. 5 we present from left to right the raw images obtained from tomography, a transversal cut obtained from Nrecon and finally the obtained image from Matlab 2020® that was used to calculated the porosity.

Porosity values obtained through tomographic image analysis show a decreasing trend as TSC increases, indicating structural compaction during drying. The exception is the limed sample (Gb_L), which maintained an almost constant porosity throughout the process. Fig. 6 illustrates the porosity evolution for each sample. Notably, Gb_L exhibited the lowest initial porosity, likely due to the mixing process with lime using a screw conveyor, which may partially disrupt the DSS structure.

The TSC value at which porosity begins to decrease corresponds closely to the onset of the S-P identified by other methods. However, unlike mechanical and rheological indicators, porosity does not recover after the S-P ends, instead, it continues to decline progressively throughout the drying process.

Microtomography is a valuable tool for tracking the structural evolution of DSS throughout the drying process. However, we do not recommend microtomography as a standalone method for identifying the sticky phase (S-P), because the porosity data alone do not capture the dynamic mechanical transitions observed with other techniques. In particular, porosity sharply decreases at the onset of drying and then remains low and stable throughout, failing to reflect the peak and resolution of the sticky phase as detected via TPA, penetrometry, or rheology.

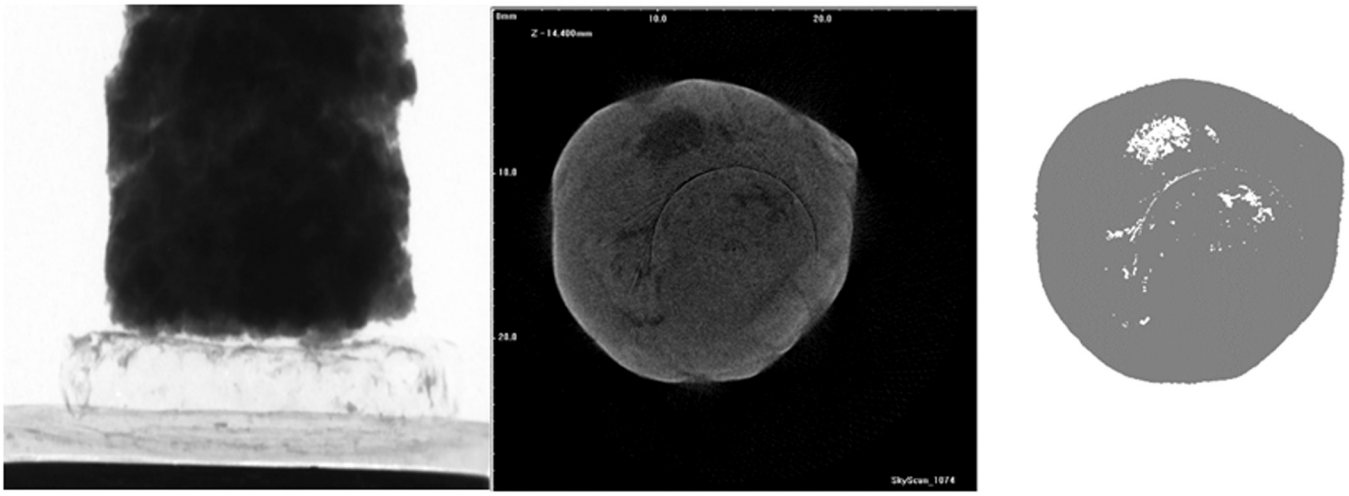

Fig. 5. Images before and after processing.

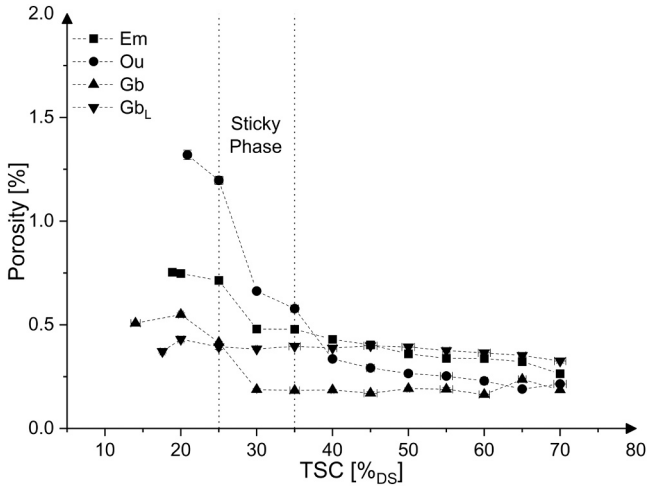

Fig. 6. Evolution of closed porosity during drying of DSS samples.

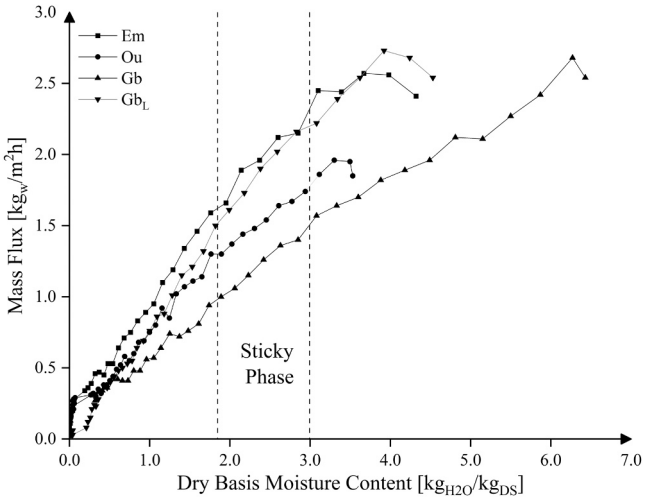

Fig. 7. Obtained Pseudo Krischer's curve for DSS samples.

3.4. Drying results

The drying experiments aimed to assess the behaviour and efficiency of DSS drying. The evaporation rate [kg_{H_2O}/h] was calculated and normalized by transfer area of the aluminium container to obtain the drying flux [kg_{H_2O}/m^2h], which was then plotted against dry basis water content [kg_{H_2O}/kg_{DS}] to generate pseudo Krischer's curves. This method, commonly used in drying studies, provides insight into the drying dynamics of the samples [39–42]. The experimental Krischer's curves obtained for the samples are shown in Fig. 7.

Gb_L exhibited the highest drying flux throughout most of the process, followed closely by Em. This enhanced performance for Gb_L may be attributed to the liming treatment, which, according to both penetration tests and TPA results, reduced adhesiveness and destabilized the S-P. Additionally, microtomography showed that Gb_L maintained a relatively constant porosity, which may have contributed to more efficient vapor escape and improved drying rates. In contrast, the Ou sample consistently showed the lowest drying flux, which aligns with its higher A/C ratio and more stable S-P as seen in the mechanical and rheological tests. Obtained results are aligned with the existing literature, which indicates that more structured DSS dries faster and shows that DSS viscoelastic properties of have a direct influence on its thermal drying [43–46],

Interestingly, although Gb and Gb_L started with similar drying rates, Gb's flux plateaued earlier and dropped more sharply, which is consistent with the increased cohesiveness and stronger S-P behaviour observed in both TPA and penetration tests. This supports the idea that DSS with a more pronounced S-P (A/C ratio) suffers greater mass transfer limitations as drying progresses.

The drying curves exhibited a clear S-P interval between 1.85 and 3.0 $kgH_2O/kgDS$ (Fig. 7, dashed lines). Table 3 summarizes the slopes of the pseudo-Krischer curves before, during, and after S-P for each sample.

Table 3
Evolution of the pseudo-Krischer curve slope (%) before, during, and after the sticky phase for each DSS sample.

	Krischer's curve slope			
Krischer's curve Phase	**Em**	**Ou**	**Gb**	**Gb_L**
Before S-P	16.1 %	23.7 %	34.9 %	14.4 %
During S-P	56.8 %	60.3 %	61.7 %	54.6 %
After S-P	65.9 %	64.4 %	68.8 %	60.0 %

4. Discussion

4.1. About the found sticky phase and its influence in DSS drying

During thermal drying, DSS samples exhibit a distinct S-P, typically within the 20–35 % DS range. This interval is characterized by transient elevations in adhesiveness relative to cohesiveness, reflected by peaks in the A/C ratio (20 % for TPA and 25 % in penetrometry for all samples except the limed sludge), and a plateau in the storage modulus (G′) at the viscoelastic limit. In this phase, the material is notably plastic and tacky, resulting in compromised flowability and operational challenges [27,47,48].

The development of the S-P, detected as an A/C peak, is attributed to moisture-induced plasticization of the sludge's organic matrix. Proteins, polysaccharides, and extracellular polymeric substances (EPS) present in the DSS form highly hydrated networks that bind water via both hydrogen bonds and hydrophobic interactions [49,50]. At high moisture, water functions as a lubricant, maintaining polymer mobility. As solids concentrate, polymer chains increasingly entangle and the network resists deformation, which manifests as heightened adhesiveness [35,51]. Upon crossing a critical dryness threshold, molecular mobility rapidly declines, the network collapses, and cohesiveness begins to predominate, marking the transition to a more brittle solid [27,49,51].

As mentioned in the introduction, the position and intensity of the S-P depends strongly on sludge composition, origin, and conditioning. In this study, the VS content was found to be a major controlling factor. Sludges rich in organic matter (Ou and Gb) exhibited a broader and earlier S-P, starting at lower total solid contents, this can be explained due to the abundance of hydrated biopolymers facilitated matrix formation and water retention, enhancing stickiness up to a critical dryness., aligning the obtained results with the literature [49,52].

In contrast, the limed sample (Gb_L), with lower VS content, displayed a narrower, weaker S-P shifted toward higher dryness levels. Liming promotes floc aggregation and increases rigidity, reducing the capacity for polymer entanglement and thus limiting adhesive behavior [53]. These trends agree with reports that lower organic content or chemical conditioning attenuate and delay the S-P during drying [43–45,54].

Porosity evolution closely follows these transitions. As water evaporates, sludge matrix contraction and pore network collapse result in a rapid decrease in porosity, a process primarily driven by capillary forces and the loss of liquid-supported structure. As drying advances, EPS rich matrices compact further, reducing pore size and total volume [38,44,55]. Once the majority of water is removed, the matrix reaches a "minimum porosity" that reflects the stable, final arrangement of solids; further drying leads to minimal additional reduction, a trend confirmed both in our data and literature pore size studies [56].

Limed sludge (GbL) behaves differently: lime addition promotes particle aggregation, stabilizes the microstructure, and preserves persistent channels that resist collapse even as water is lost [43–45,54]. Thus, porosity stabilizes after initial contraction, particularly in conditioned sludges where such persistent pathways facilitate vapor escape and maintain permeability

These findings underscore the close connection between compositional features, mechanical properties, and drying performance. Our integration of texture analysis, rheology, and microstructural characterization enables precise identification of the sticky phase and quantifies its impact on sludge handling and dryer efficiency. Such insights are crucial for improving process strategies—such as optimizing conditioning, mixing, or drying protocols, to mitigate stickiness, reduce energy costs, and enhance operational robustness in wastewater treatment facilities.

Interpretation of the drying flux behaviour confirms that the sticky phase (S-P), identified by TPA and penetration testing, represents a key threshold in DSS dewatering [57,58]. As samples pass through the S-P interval as show in Fig. 7 and Table 3 the slope of the Krischer curve steepens considerably, indicating a rapid increase in resistance to moisture transfer caused by matrix densification, pore collapse, and biopolymer network rearrangement [47,59]. Crucially, this elevated resistance does not recover after the interval; the post-S-P slopes remain high, demonstrating that once these microstructural transitions occur, they irreversibly limit water mobility. This mechanistic irreversibility is consistent with previous studies, which show that after the sticky phase, the sludge drying curve remains steep, and further drying becomes increasingly energy-intensive [17,60].

4.2. Evaluation of tested methods in the evolution of DSS textural and viscoelastic properties during drying

Fig. 8 summarizes the TSC ranges over which each of the four applied methods (TPA, penetrometry, oscillatory rheology, and microtomography) were successfully implemented, alongside the corresponding textural states of the DSS. This visual overview enables a clear evaluation of each method's applicability throughout the drying process and highlights their respective operational limits.

The Texture Profile Analysis (TPA) method was effective during the viscoelastic-pasty phase, approximately between 15 % and 40 $\%_{DS}$. This test requires that DSS samples be extruded into stable cylindrical shapes capable of withstanding two compression cycles. Therefore, it is not recommended for samples with low TSC (highly fluid) or those above 40 $\%_{DS}$, where cylinders end to crack or collapse during testing, compromising result reliability. Despite these limitations, TPA was particularly valuable for detecting the S-P, notably through distinct peaks in the adhesiveness-to-cohesiveness (A/C) ratio.

Penetrometry was the most versatile technique, operating reliably from 20 to over 80 $\%_{DS}$, covering the entire viscoelastic-pasty and solid phases. It was especially useful in mapping the S-P and assessing mechanical resistance across the full drying range. The S-P could be identified through a characteristic peak in the A/C ratio, similar to TPA but applicable over a broader dryness interval.

Oscillatory rheology was applicable from 15 % to 45 $\%_{DS}$, offering valuable insight into the viscoelastic behaviour of DSS, including the evolution of the storage modulus at the viscoelastic limit. However, beyond 50 $\%_{DS}$, the presence of rigid solids interfered with measurement accuracy and posed potential risks to the equipment. In this case, the S-P was identified by a plateau in the storage modulus, suggesting a temporary stabilization in the material's internal structure.

Microtomography served as a complementary technique by tracking porosity evolution in the DSS structure. It was applicable from 15 % to 80 $\%_{DS}$, covering nearly the entire drying trajectory. However, this method only allowed identification of the onset of the S-P, marked by a noticeable drop in porosity. Since it does not fully capture the dynamics of the S-P, it is recommended to use microtomography as a supporting technique in conjunction with TPA, penetrometry, or rheology.

Crucially, the S-P was consistently detected between 20 % and 35 $\%_{DS}$, as confirmed by all applicable methods. The convergence of these independent techniques reinforces the robustness of this interval and highlights the importance of a multi-method approach for accurately monitoring and characterizing this critical drying stage in DSS processing.

While the sticky phase identified in this study (20–35 $\%_{DS}$) aligns with several previous findings, it is important to note that this interval may vary significantly depending on sludge origin, treatment history, composition (e.g., organic matter, sand content), and environmental factors (see Table 1). Therefore, we recommend that treatment facilities or researchers characterize the sticky phase of their specific sludge using one or more of the validated methods outlined in this study. Doing so can support better process control and more efficient dryer design tailored to the unique behaviour of each sludge type.

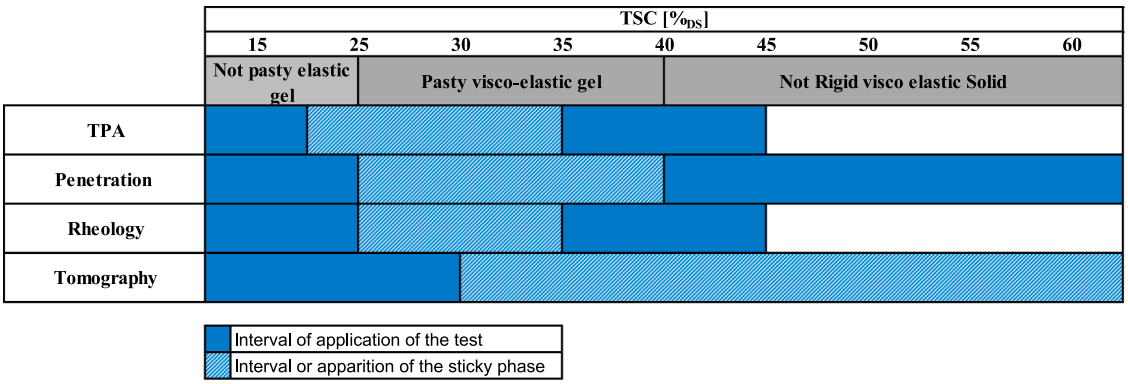

Fig. 8. Summary of applicability of studied test in the evaluation of DSS textural and viscoelastic properties.

5. Conclusions

This study investigated the evolution of textural and viscoelastic properties of DSS during drying, with a particular focus on identifying and characterizing the S-P. Through the combined use of penetration testing, texture profile analysis (TPA), oscillatory rheology, and microtomography, we established consistent indicators of the S-P in the 20–35 $\%_{DS}$ total solid content (TSC) range across all samples.

Among the techniques tested, the penetration test proved to be the most robust, remaining effective across the entire dryness range. In contrast, TPA and oscillatory rheology showed limitations at higher TSC levels due to structural degradation and measurement instability, respectively. Microtomography offered valuable insights into internal porosity evolution but was only effective for detecting the onset of the S-P and not its full extent.

The influence of DSS origin and treatment conditions, especially liming, was also confirmed. Limed sludge samples exhibited lower stickiness and a less stable S-P, suggesting that lime addition can mitigate operational issues during thermal drying by altering sludge microstructure and reducing adhesion.

Overall, this work provides a multi-technique framework for identifying the S-P in DSS and highlights practical considerations for optimizing drying processes. The methodology is adaptable to various DSS types and may assist in the design and operation of more efficient drying systems.

CRediT authorship contribution statement

Léonard Angelique: Writing – review & editing, Writing – original draft, Validation, Supervision, Project administration, Investigation, Conceptualization. **Ben Hamed Hajer:** Writing – review & editing, Writing – original draft, Investigation. **Fantasse Azedinne:** Writing – review & editing, Writing – original draft, Methodology, Investigation. **Parra Angarita Sergio Luis:** Writing – review & editing, Writing – original draft, Visualization, Validation, Supervision, Software, Methodology, Investigation, Formal analysis, Data curation, Conceptualization. **Essanoussi Mohamed:** Writing – review & editing, Writing – original draft, Methodology, Investigation, Formal analysis.

Declaration of Competing Interest

The authors declare the following financial interests/personal relationships which may be considered as potential competing interests: ANGELIQUE LEONARD reports financial support was provided by Fund for Scientific Research. SERGIO LUIS PARRA ANGARITA reports financial support was provided by Fund for Scientific Research. BEN HAMED HAJED reports financial support was provided by Fund for Scientific Research. If there are other authors, they declare that they have no known competing financial interests or personal relationships that could have appeared to influence the work reported in this paper.

Acknowledgments

The authors wish to acknowledge the support of the personnel of the Chemical Engineering Halle of the University of Liège. We also extend our thanks to the FRS-FNRS (Fund for Scientific Research) for funding their research project through the grant T.0159.20-PDR. Lastly, we express our sincere appreciation to L'Association Intercommunale pour le Démergement et l'Epuration des communes de la province de Liège (AIDE) for granting permission to collect samples, which played a significant role in advancing this research.

Data Availability

Data are contained within the article

References

[1] Ben Hamed H, Debuigne A, Kleinjan H, Toye D, Léonard A. Enhancing sewage sludge stabilization, pathogen removal, and biomass production through indigenous microalgae promoting growth: a sustainable approach for sewage sludge treatment. Recycling 2024;9. https://doi.org/10.3390/recycling9050097.
[2] Eurostat. Population connected to wastewater treatment facilities (2018). Popul Connect Wastewater Treat Plants 2021:1. https://doi.org/10.1787/eb0d56f0-en.
[3] Ferrentino R., Langone M., Fiori L.Full-Scale Sewage Sludge Reduction Technologies: A Review with a Focus on Energy Consumption; 2023, 1-20.
[4] Chang H., Zhao Y., Xu A., Damgaard A., Christensen T.H., Mini-review of inventory data for the dewatering and drying of sewage sludge; 2023, 10.1177/0734242X221139170.
[5] Eshtiaghi N, Markis F, Yap SD, Baudez JC, Slatter P. Rheological characterisation of municipal sludge: a review. Water Res 2013;47:5493–510. https://doi.org/10.1016/j.watres.2013.07.001.
[6] Infusino E, Caloiero T. Municipal wastewater sludge rheology: impact of temperature, solid content, and settling solids. Water Environ Res 2021;93:2971–81. https://doi.org/10.1002/wer.1646.
[7] Feng G, Hu Z, Ma H, Bai T, Guo Y, Hao Y. Semi-solid rheology characterization of sludge conditioned with inorganic coagulants. Water Sci Technol 2019;80:2158–68. https://doi.org/10.2166/wst.2020.022.
[8] Peeters B. Effect of activated sludge composition on its dewaterability and sticky phase. Fac Eng Dep Chem Eng Leuven 2011.
[9] Yen PS, Chen LC, Chien CY, Wu RM, Lee DJ. Network strength and dewaterability of flocculated activated sludge. Water Res 2002;36:539–50. https://doi.org/10.1016/S0043-1354(01)00260-3.
[10] Peeters B, Dewil R, Van Impe JF, Vernimmen L, Smets IY. Using a shear test-based lab protocol to map the sticky phase of activated sludge. Environ Eng Sci 2011;28:81–5. https://doi.org/10.1089/ees.2010.0168.
[11] Liang F, Sauceau M, Dusserre G, Arlabosse P. A uniaxial cyclic compression method for characterizing the rheological and textural behaviors of mechanically dewatered sewage sludge. Water Res 2017;113:171–80. https://doi.org/10.1016/j.watres.2017.02.008.
[12] Li B, Wang F, Chi Y, Yan JH. Adhesion and cohesion characteristics of sewage sludge during drying. Dry Technol 2014;32:1598–607. https://doi.org/10.1080/07373937.2014.910522.
[13] Mouzaoui M, Sauceau M, Devriendt L, Baudez JC, Arlabosse P. Rheological characterization of sludge in divided granular-like and pasty states using a granular rheometer. Powder Technol 2021;378:521–7. https://doi.org/10.1016/j.powtec.2020.09.070.

[14] Mouzaoui M, Baudez JC, Sauceau M, Arlabosse P. Experimental rheological procedure adapted to pasty dewatered sludge up to 45% dry matter. Water Res 2018;133:1–7. https://doi.org/10.1016/j.watres.2018.01.006.
[15] Durdevic D, Zikovich S, Blecich P. Sustainable sewage sludge management technologies selection based on techno-economic-environmental criteria: case study of croatia. Energies 2022;15:3941.
[16] Rao B, Wang G, Xu P. Recent advances in sludge dewatering and drying technology. Dry Technol 2022;40:3049–63. https://doi.org/10.1080/07373937.2022.2043355.
[17] Léonard A, Vandevenne P, Salmon T, Marchot P, Crine M. Wastewater sludge convective drying: Influence of sludge origin. Environ Technol 2004;25:1051–7. https://doi.org/10.1080/09593330.2004.9619398.
[18] Peeters B, Dewil R, Vernimmen L, Van den Bogaert B, Smets IY. Addition of polyaluminiumchloride (PACl) to waste activated sludge to mitigate the negative effects of its sticky phase in dewatering-drying operations. Water Res 2013;47:3600–9. https://doi.org/10.1016/j.watres.2013.04.012.
[19] Chen X, Huang X, Tan H, Li Y, Cao H, Jin Y, et al. Effect of sand content on adhesion and cohesion of municipal sludge during drying practices: the characteristics and modification. Dry Technol 2024;42:2268–77. https://doi.org/10.1080/07373937.2024.2419000.
[20] Kudra T. Sticky region in drying - Definition and identification. Dry Technol 2003;21:1457–69. https://doi.org/10.1081/DRT-120024678.
[21] Arlabosse P, Chavez S, Prevot C. Drying of municipal sewage sludge: from a laboratory scale batch indirect dryer to the paddle dryer. Braz J Chem Eng 2005;22:227–32. https://doi.org/10.1590/S0104-66322005000200009.
[22] Ruiz T, Kaosol T, Wisniewski C. Dewatering of urban residual sludges: filterability and hydro-textural characteristics of conditioned sludge. Sep Purif Technol 2010;72:275–81. https://doi.org/10.1016/j.seppur.2010.02.017.
[23] Li H, Zou S, Li Y, Jin Y. Characteristics and model of sludge adhesion during thermal drying. Environ Technol 2013;34:807–12. https://doi.org/10.1080/09593330.2012.720614.
[24] Deng WY, Yuan MH, Mei J, Liu YJ, Su YX. Effect of calcium oxide (CaO) and sawdust on adhesion and cohesion characteristics of sewage sludge under agitated and non-agitated drying conditions. Water Res 2017;110:150–60. https://doi.org/10.1016/j.watres.2016.12.001.
[25] Deng W, Xiao J, Lai Z, Su Y. A new method to characterize sludge stickiness during drying: Effects of sludge temperature and calcium oxide (CaO) on stickiness. Dry Technol 2020;38:1107–20. https://doi.org/10.1080/07373937.2019.1615938.
[26] Mupinga RT, Septien S, Pocock J, Buckley CA. An investigation into the stickiness of faecal sludge: Preliminary investigation of VIP and UDDT sludge with varying moisture content at ambient temperature. Gates Open Res 2020;4:78.
[27] Mupinga RT, Mercer E, Rayavellore Suryakumar A, Pocock J, Septien S. Insight into the stickiness of faecal sludge from dry sanitation technologies: a path toward sustainable and efficient FSM via thermal processes. Results Eng 2025;26:105453. https://doi.org/10.1016/j.rineng.2025.105453.
[28] Pambou YB, Fraikin L, Salmon T, Crine M, Léonard A. Sludge dewatering and drying: about the difficulty of making experiments with a non-stabilized material. Desalin Water Treat 2016;57:13841–56. https://doi.org/10.1080/19443994.2015.1060534.
[29] Chambers P. Standard methods for the examination of water and wastewater. Scientific e-Resources; 2019.
[30] Pambou Y.-B. Influence du conditionnement et de la déshydratation mécanique sur le séchage des boues d'épuration; 2016.
[31] Parra-Angarita SL, Al Sayed MW, Léonard A. The variability of textural properties and drying characteristics of dehydrated sewage sludge. Clean Technol 2025;7. https://doi.org/10.3390/cleantechnol7020031.
[32] Collivignarelli MC, Carnevale Miino M, Bellazzi S, Caccamo FM, Durante A, Abbà A. Review of rheological behaviour of sewage sludge and its importance in the management of wastewater treatment plants. Water Pr Technol 2022;17:483–91. https://doi.org/10.2166/wpt.2021.098.
[33] Seyssiecq I, Ferrasse JH, Roche N. State-of-the-art: rheological characterisation of wastewater treatment sludge. Biochem Eng J 2003;16:41–56. https://doi.org/10.1016/S1369-703X(03)00021-4.
[34] Nishinari K, Kohyama K, Kumagai H, Funami T, Bourne MC. Parameters of texture profile analysis. Food Sci Technol Res 2013;19:519–21. https://doi.org/10.3136/fstr.19.519.
[35] Ayol A, Dentel SK, Filibeli A. Toward efficient sludge processing using novel rheological parameters: dynamic rheological testing. Water Sci Technol 2006;54:17–22. https://doi.org/10.2166/wst.2006.542.
[36] Feng G, Tan W, Zhong N, Liu L. Effects of thermal treatment on physical and expression dewatering characteristics of municipal sludge. Chem Eng J 2014;247:223–30. https://doi.org/10.1016/j.cej.2014.03.005.
[37] Marinetti M, Dentel SK, Malpei F, Bonomo L. Assessment of rheological methods for a correlation to sludge filterability. Water Res 2010;44:5398–406. https://doi.org/10.1016/j.watres.2010.06.046.
[38] Léonard A, Blacher S, Marchot P, Pirard JP, Crine M. Image analysis of X-ray microtomograms of soft materials during convective drying: 3D measurements. J Microsc 2005;218:247–52. https://doi.org/10.1111/j.1365-2818.2005.01485.x.
[39] Pambou YB, Fraikin L, Salmon T, Crine M, Léonard A. Enhanced sludge dewatering and drying comparison of two linear polyelectrolytes co-conditioning with polyaluminum chloride. Desalin Water Treat 2016;57:27989–8006. https://doi.org/10.1080/19443994.2016.1178602.
[40] Tsotsas E., Mujumdar A.S. Modern Drying Technology Edited by Evangelos Tsotsas and Arun S. Mujumdar; 2007.
[41] Bennamoun L, Arlabosse P, Léonard A. Review on fundamental aspect of application of drying process to wastewater sludge. Renew Sustain Energy Rev 2013;28:29–43. https://doi.org/10.1016/j.rser.2013.07.043.
[42] Zheng Q, Hu Z, Li P, Ni L, Huang G, Yao Y, et al. Effects of air parameters on sewage sludge drying characteristics and regression analyses of drying model coefficients. Appl Therm Eng 2021;198:117501. https://doi.org/10.1016/j.applthermaleng.2021.117501.
[43] Léonard A, Royer S, Blandin G, Salmon T, Fraikin L, Crine M. Importance of mixing conditions during sludge liming prior to their convective drying. Eur Dry Conf Palma Spain 2011:26–8.
[44] Huron Y, Salmon T, Crine M, Blandin G, Léonard A. Effect of liming on the convective drying of urban residual sludges. AsiaPac J Chem Eng 2010;5:909–14. https://doi.org/10.1002/apj.421.
[45] Li H, Zou S, Li C. Liming pretreatment reduces sludge build-up on the dryer wall during thermal drying. Dry Technol 2012;30:1563–9. https://doi.org/10.1080/07373937.2012.697947.
[46] Li J, Fraikin L, Salmon T, Bennamoun L, Toye D, Schreinemachers R, et al. Investigation on convective drying of mixtures of sewage sludge and sawdust in a fixed bed. Dry Technol 2015;33:704–12. https://doi.org/10.1080/07373937.2014.982254.
[47] Peeters B, Dewil R, Smets I. Challenges of drying sticky wastewater sludge. Chem Eng 2014;121.
[48] Kiang Y-H. Biosludge drying: system design schemes for the sticky phase. Chem Eng 2018;125.
[49] Yoo J, Oshita K, Kusakabe T, Takaoka M. Adhesion behavior of dewatered sewage sludge during indirect thermal drying. J Environ Manag 2025;381:125203. https://doi.org/10.1016/j.jenvman.2025.125203.
[50] Ye ZL, Lu HW, Gao X, Liu JQ, Jin Y. Research progress of micro-CT in the field of petroleum engineering. Springe Ser Geomech Geoengin 2024:726–38. https://doi.org/10.1007/978-981-97-0468-2_55.
[51] Eslami Z, Elkoun S, Robert M, Adjallé K. A review of the effect of plasticizers on the physical and mechanical properties of alginate-based films. Molecules 2023;28. https://doi.org/10.3390/molecules28186637.
[52] Léonard A, Blandin G, Crine M. Importance of rheological properties when drying sludge in a fixed bed. Lab Chem Eng Univ 2014;III:102–50.
[53] Yu W, Yang J, Shi Y, Song J, Shi Y, Xiao J, et al. Roles of iron species and pH optimization on sewage sludge conditioning with Fenton's reagent and lime. Water Res 2016;95:124–33. https://doi.org/10.1016/j.watres.2016.03.016.
[54] Hil A, Judenne E, Remy M. The effect of lime treatment on sludge rheological properties. Technology 2005:1–6.
[55] Léonard A, Blacher S, Pirard R, Marchot P, Pirard JP, Crine M. Multiscale texture characterization of wastewater sludges dried in a convective rig. Dry Technol 2003;21:1507–26. https://doi.org/10.1081/DRT-120024490.
[56] Liu J, Liu H, He C, Xiao H, Jin M, Yao H. Correlation between sewage sludge pore structure evolution and water filtration performance: effect of thermal hydrolysis with or without carbonaceous skeleton-assisted. Water Res 2025;268:122578. https://doi.org/10.1016/j.watres.2024.122578.
[57] Zhang Q, Wang B, Xing Y, Wang G, Zhang X, Lü X. Drying characteristics of sewage sludge pre-conditioned by CaO and sawdust under low-temperature drying conditions. Environ Technol 2024;45:6237–48. https://doi.org/10.1080/09593330.2024.2330474.
[58] Mujumdar AS, Tsotsas E. Modern drying technology. Wiley-VCH; 2007.
[59] Wang HF, Ma YJ, Wang HJ, Hu H, Yang HY, Zeng RJ. Applying rheological analysis to better understand the mechanism of acid conditioning on activated sludge dewatering. Water Res 2017;122:398–406. https://doi.org/10.1016/j.watres.2017.05.002.
[60] Li J, Fraikin L, Salmon T, Toye D, Léonard A. Influence of back-mixing on the convective drying of sewage sludge: the structural characteristics. Dry Technol 2022;40:205–12. https://doi.org/10.1080/07373937.2020.1781159.